Center for Turbulence Research
Proceedings of the Summer Program 1988

Phase decorrelation, streamwise vortices and acoustic radiation in mixing layers

By C. M. Ho[1], Y. Zohar[1], R.D. Moser[2], M.M. Rogers[2], S.K. Lele[3] AND J.C. Buell[2]

Several direct numerical simulations have been performed and analyzed to study various aspects of the early development of mixing layers. Included are (1) the phase jitter of the large-scale eddies, which was studied using a two-dimensional spatially-evolving mixing layer simulation; (2) the response of a time-developing mixing layer to various spanwise disturbances; and (3) the sound radiation from a two-dimensional compressible time-developing mixing layer.

1. Phase decorrelation in a spatially-developing mixing layer

Since the realization that spanwise coherent structures (rolls) dominate the dynamics of free shear flows, much effort has been focused on the control of these rolls in an effort to manipulate shear layers (Ho & Huerre 1984). When low-level periodic excitation is applied to force a mixing layer, the vortex formation becomes phase-locked with the forcing signal. However, experiments by Zohar et al. (1988) show that a short distance from the splitter-plate trailing-edge, the phase jitter increases abruptly indicating the loss of phase correlation. To achieve better control of the mixing layer it is important to understand the cause of this phase jitter.

The phase decorrelation of the spanwise rolls was studied using a 2-D numerical code written for spatially-developing free shear flows. The code is based on a spectral method in the vertical direction (which extends to infinity) and high-order compact finite differencing in the streamwise direction. The advantage of numerical simulations over experiments is that some possible causes of the phase decorrelation, such as 3-D effects or small-scale transition, can be isolated. A simulation was performed at a Reynolds number of 100, with 1% forcing of the inlet vertical velocity at a frequency of 0.18. (The length and velocity scales are the initial vorticity thickness and free stream velocity difference.) The velocity ratio is $R = (U_1 - U_2)/(U_1 + U_2) = 2/3$. As documented elsewhere, the inflow and outflow boundary conditions lead to feedback from the latter to the former through the pressure. This has the net effect of introducing a small amount of noise into the

1 University of Southern California
2 NASA Ames Research Center
3 Center for Turbulence Research

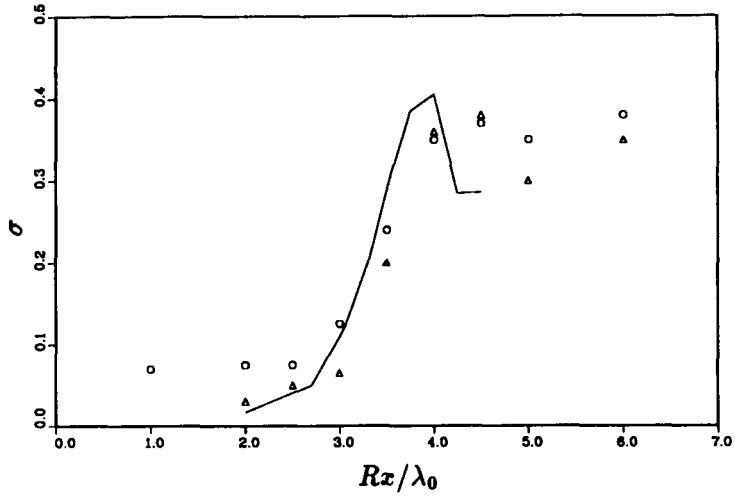

FIGURE 1. Standard deviation of the difference between successive zero crossing (σ) as a function of down-stream distance. Current results, ——— ; Experiments of Zohar *et al.*, △ , forced, o natural.

system at the inflow boundary. We believe the results should be independent of the origin of the noise, although in the present case the noise is not random.

The numerical results quantitatively confirm the experimental data, as shown in figure 1. The standard deviation of the difference between successive zero crossings of the v-velocity is plotted as a function of the downstream distance. The phase jitter of the passing coherent rolls increases sharply around the first vortex merging. Therefore, the phase jitter is primarily a 2-D phenomenon, and neither phase instability nor small-scale transition is the cause of it. The frequency spectrum of the velocity fluctuations, shown in figure 2, indicates that the contamination of the subharmonic mode by background noise is responsible for the loss of the phase information. The subharmonic mode is amplified as an unstable mode from the noise via energy transfer from the fundamental. Consequently, the resulting paired rolls are not phase-locked with the forcing signal.

2. Three-dimensional temporally-evolving mixing layers

Plan-view shadowgraph pictures taken by Konrad (1976) clearly reveal the existence of periodically distributed streamwise streaks, positioned in the braid region between the large coherent spanwise rollers of their mixing layer. These streaks are a result of counterrotating pairs of streamwise vortices (Bernal & Roshko 1986) that arise from a secondary instability of the plane mixing layer. Pierrehumbert & Widnall (1982) have used linear stability analysis to show that the most amplified spanwise wavelength is about 2/3 of the streamwise wavelength of the large coherent rollers for a class of Stuart (1967) vortices with a vorticity distribution similar to that of experimental mixing layers. They also found that the growth-rate curve is fairly flat around this most amplified wavelength. This wavelength ratio is in good

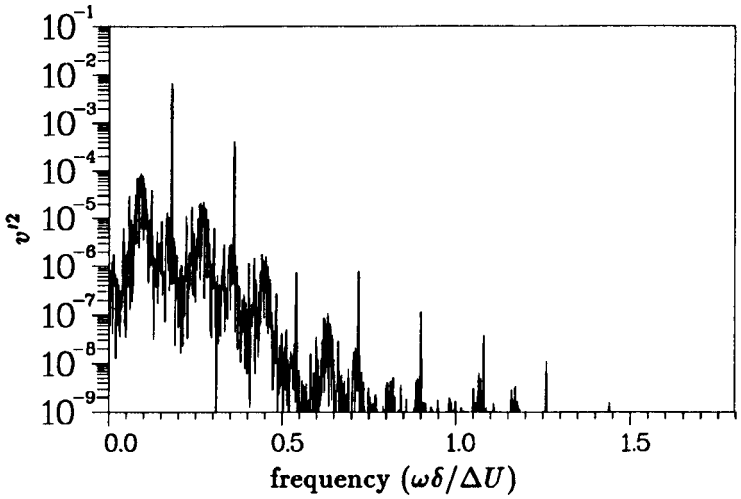

FIGURE 2. Spectrum of the cross-stream velocity (v) at $x/\delta = 140$ and $y = 0$.

agreement with that of experimentally observed structures and was also found to remain constant after the merging or pairing of the coherent rolls (Huang & Ho 1988). The mechanism by which this ratio remains constant during a pairing (i.e., how the spacing of the streamwise vortices doubles) is not understood.

A three-dimensional temporally-evolving shear layer code was used to study the development of mixing layers in the presence of spanwise disturbances. The temporal nature of the simulation permits the direct use of spectral methods in the periodic streamwise and spanwise directions. The cross-stream direction is mapped onto a uniform grid in a finite domain using a cotangent mapping and the spatial dependence of each dependent variable in this direction is represented by a Fourier series in the mapped domain (see Cain, Ferziger & Reynolds 1984).

In order to estimate the most unstable spanwise wavelength of a mixing layer during both roll up and pairing the code was modified to ensure that the three-dimensional disturbances remained small (and thus could be treated as linear). This rescaling of the disturbance in no way affects the development of the two-dimensional base flow. The spanwise periodic boundary condition requires that all spanwise disturbances must have an integral number of wavelengths in the computational domain. In order to permit a "natural" wavelength selection it is thus necessary to use a very large spanwise computational domain compared to the expected most unstable spanwise wavelength. This will ensure that the flow can select the wavelength of its choice rather than one imposed by the computational box. Each spanwise wavenumber is initialized with a small disturbance and the growth (or decay) rate of the disturbance in each wavenumber is recorded as the two-dimensional mixing layer undergoes first a roll up and then a pairing. The initial streamwise disturbances used were eigenfunctions determined from inviscid linear theory (Rayleigh eigenfunctions).

Plots of the growth rate of each spanwise wavenumber at two times in the mixing

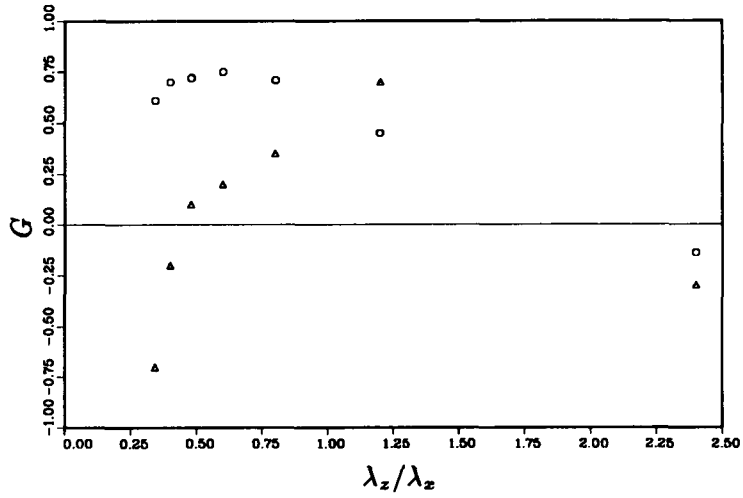

FIGURE 3. Growth rates (G) of Fourier modes of with spanwise wave-length λ_z at two times: o , roll up ($t = 16\delta/U$) and $\triangle$, pairing ($t = 25.5\delta/U$).

layer development are shown in figure 3. At early time, when the layer has rolled up but not yet paired, the most unstable wavelength is about 60% of the streamwise wavelength. When vortex pairing occurs, the amplified band of streamwise vortex disturbances shifts toward longer wavelengths, as can be seen in figure 3. The most amplified wavelength is then about twice the wavelength before pairing. Thus the most amplified wavelength of the streamwise vortices remains proportional to the local wavelength of the coherent structures, in agreement with the experimental observations.

This analysis suggests a mechanism by which the experimentally observed spanwise scale change could occur at a pairing; that is, the longer wavelength modes begin to grow faster than the mode at the originally dominant scale. However, there are two major shortcomings of the analysis. The first is that it is linear, and there may be important non-linear effects. The second is that only local (in time) growth rates are considered, whereas the observed strength of a given Fourier mode depends on the time-integral of the growth.

To address these difficulties, a fully non-linear computation was performed. This simulation was done using an improved numerical method based on a hyperbolic tangent mapping of the cross-stream (y) coordinate. The simulation was initialized with an array of weak streamwise vortices corresponding to the most unstable spanwise wavelength (60% of the streamwise wavelength). The subharmonic in the spanwise direction was also excited but at half the amplitude. It is this subharmonic which should grow to become dominant if there is to be a scale change after a pairing. Energies in four of the Fourier modes in the simulation are shown as a function of time in figure 4. The fundamental and subharmonic of the main Kelvin-Helmholtz roll up ($k_z = 0$) are shown indicating the time at which roll up (when the fundamental is maximum) and pairing (when the subharmonic is maximum)

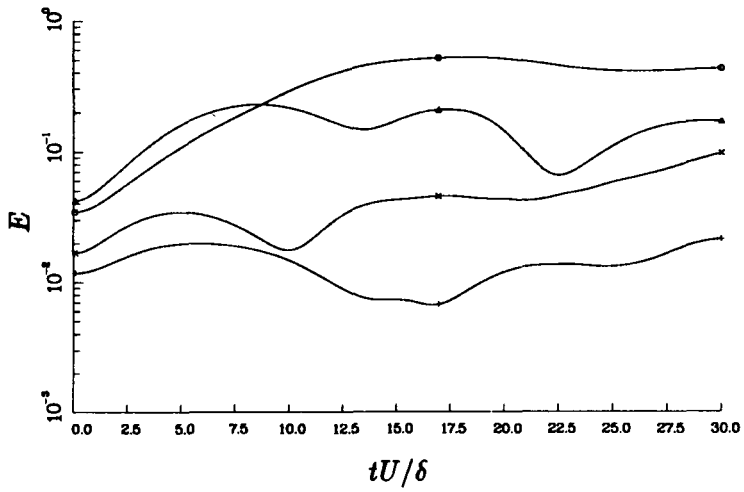

FIGURE 4. Evolution of the energy in four Fourier modes: △ , fundamental Kelvin-Helmholtz mode, ○ subharmonic Kelvin-Helmholtz mode, × fundamental streamwise vortex mode, + , subharmonic streamwise vortex mode.

occur. Note that the subharmonic of the mode representing the streamwise vortices ($k_x = 0$), does not grow or become dominant after the pairing. Thus there is no indication of a spanwise scale change in this simulation. The reason for the discrepancy between the fully non-linear simulation and both the experimental observations and linear analysis is not known. This is a problem for future research.

Another form of spanwise disturbance that was studied consists of a spanwise variation of the vorticity thickness. Such flows could be difficult to realize in the laboratory and numerical simulation provides a good means to study their behavior.

Several simulations were made using an initially sinusoidal spanwise variation (one period in the computational domain) of vorticity thickness with a maximum to minimum thickness ratio of two. As before, initial streamwise disturbances were determined from inviscid stability theory. The spanwise extent of the computational box was five times the wavelength of the most unstable mode in the initially thin region of the layer. When forced by the eigenfunction associated with the most unstable frequency of the layer at its thinnest point, roll up was observed to occur only in this region. Further simulations were made with the addition of an eigenfunction at the subharmonic frequency at various phases relative to the fundamental. In these cases the layer rolled up and paired at the thin location while a roll up occurred at the thick location, ultimately leading to one spanwise vortex (figure 5). Figure 6 shows the behavior at an earlier time. At the thin location (figure 6a) two well-defined rollers have developed in a manner similar to a two-dimensional layer with the same streamwise disturbances. At the thick location (figure 6b) a weak roll up of two vortices has started. Intermediate locations show intermediate behavior (figure 6c). Slightly later the pairing at the thin location is nearing completion as it does in the two-dimensional case. At the thick location the forward

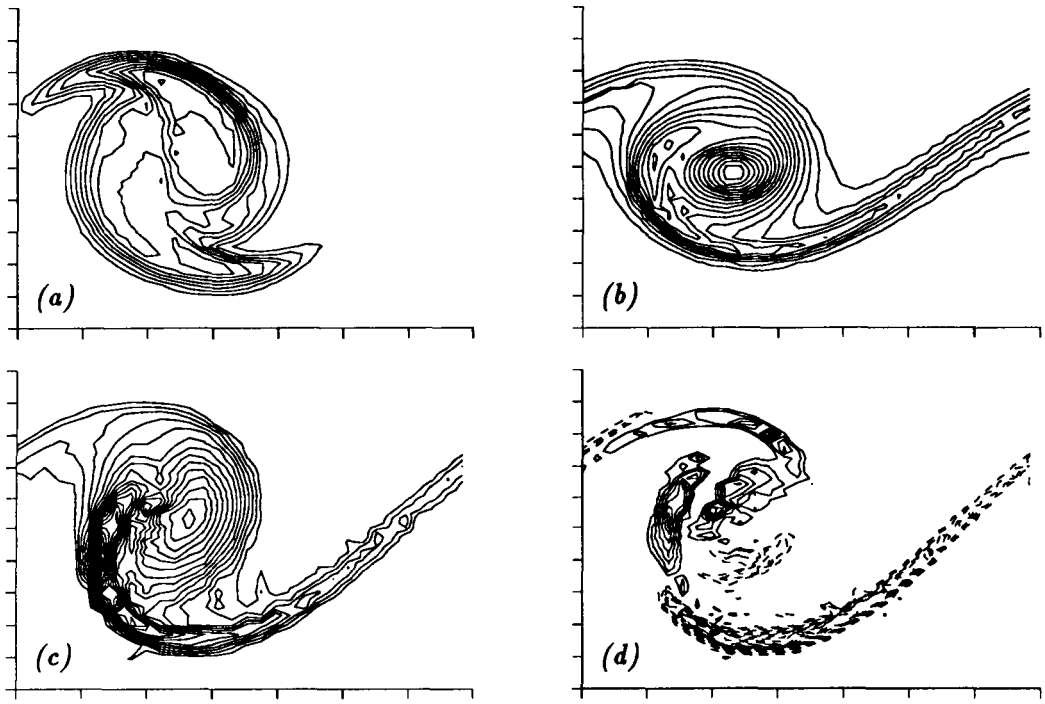

FIGURE 5. Vorticity distribution in x-y planes at a late time, $t = 19.9\delta/U$. (a) spanwise vorticity, ω_z, at the initially thin location (peak level -1.2); (b) spanwise vorticity, ω_z, at the initially thick location (peak level -1.9); (c) spanwise vorticity, ω_z, at location half way between (a) and (b) (peak level -1.8); (d) streamwise vorticity, ω_x, at same location as (c) (levels ranging from -0.7 to 0.4, dashed contours correspond to negative contour levels).

vortex lump has been almost completely absorbed by the rear vortex lump as the full roll up of figure 5b is being approached (this stage bears some resemblance to the two-dimensional "shredding" behavior observed when the fundamental and subharmonic disturbance have a relative phase that inhibits pairing). Intermediate locations are again intermediate in behavior.

During this process the blending of rollers at different locations is associated with the development of streamwise vorticity. Initially there is no streamwise vorticity anywhere in the domain and by symmetry none ever forms at the thinnest and thickest spanwise sections of the layer. In the intermediate regions, however, significant streamwise vorticity does develop. Figure 6d illustrates its form at a section half way between the thickest and thinnest locations. From this section the streamwise vorticity structure appears to resemble the streamwise vortices typical of the secondary instability described earlier. However, a three-dimensional surface plot shows that, rather than roughly axisymmetric streamwise vortices, this section represents a cut through a slab-like structure of streamwise vorticity that extends the entire width from the thinnest to thickest point of the layer. As the roll up

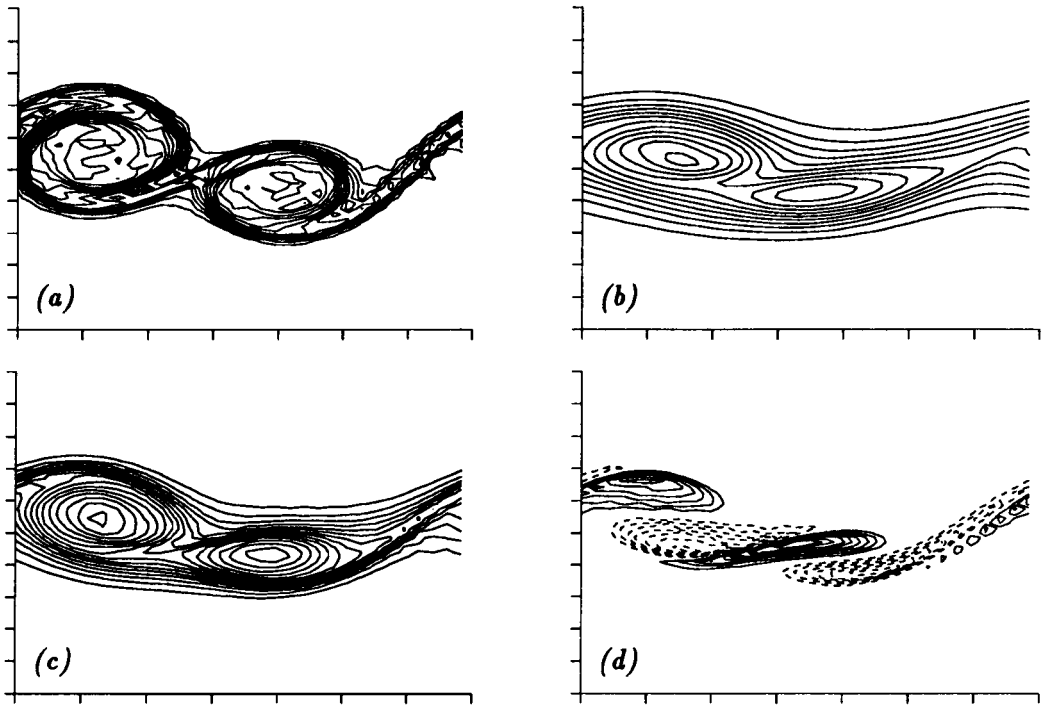

FIGURE 6. Vorticity distribution in x-y planes at an early time, $t = 12.0\delta/U$. (a) spanwise vorticity, ω_z, at the initially thin location (peak level -1.4); (b) spanwise vorticity, ω_z, at the initially thick location (peak level -1.2); (c) spanwise vorticity, ω_z, at location half way between (a) and (b) (peak level -1.5); (d) streamwise vorticity, ω_x, at same location as (c) (levels ranging from -0.45 to 0.6, dashed contours correspond to negative contour levels).

progresses at the thick location the magnitude of the streamwise vorticity increases (up to ± 1.6) but ultimately, when the layer approaches one large two-dimensional roller it decays to the moderate levels observed in figure 5d.

Future plans include the study of the more interesting case where the ratio of the vorticity thickness of the thick to the thin region is not an integer number.

3. Acoustic radiation from vortex roll up and pairing

In low Mach number shear layers, the energy radiated by sound is a small portion of that generated by turbulence production. At higher Mach numbers the sound radiation can be a major energy sink. It was suggested by Laufer (1974) that the merging of the spanwise rolls was the dominant sound generation mechanism; however, the detailed process has never been clarified. A compressible temporally-developing shear layer code was used to study this problem. The code used high-order accurate compact finite differencing. The calculation domain contained the entire region with significant pressure fluctuations, from the near-field of shear layer vortices to the far-field region. The process of noise generation was identified by

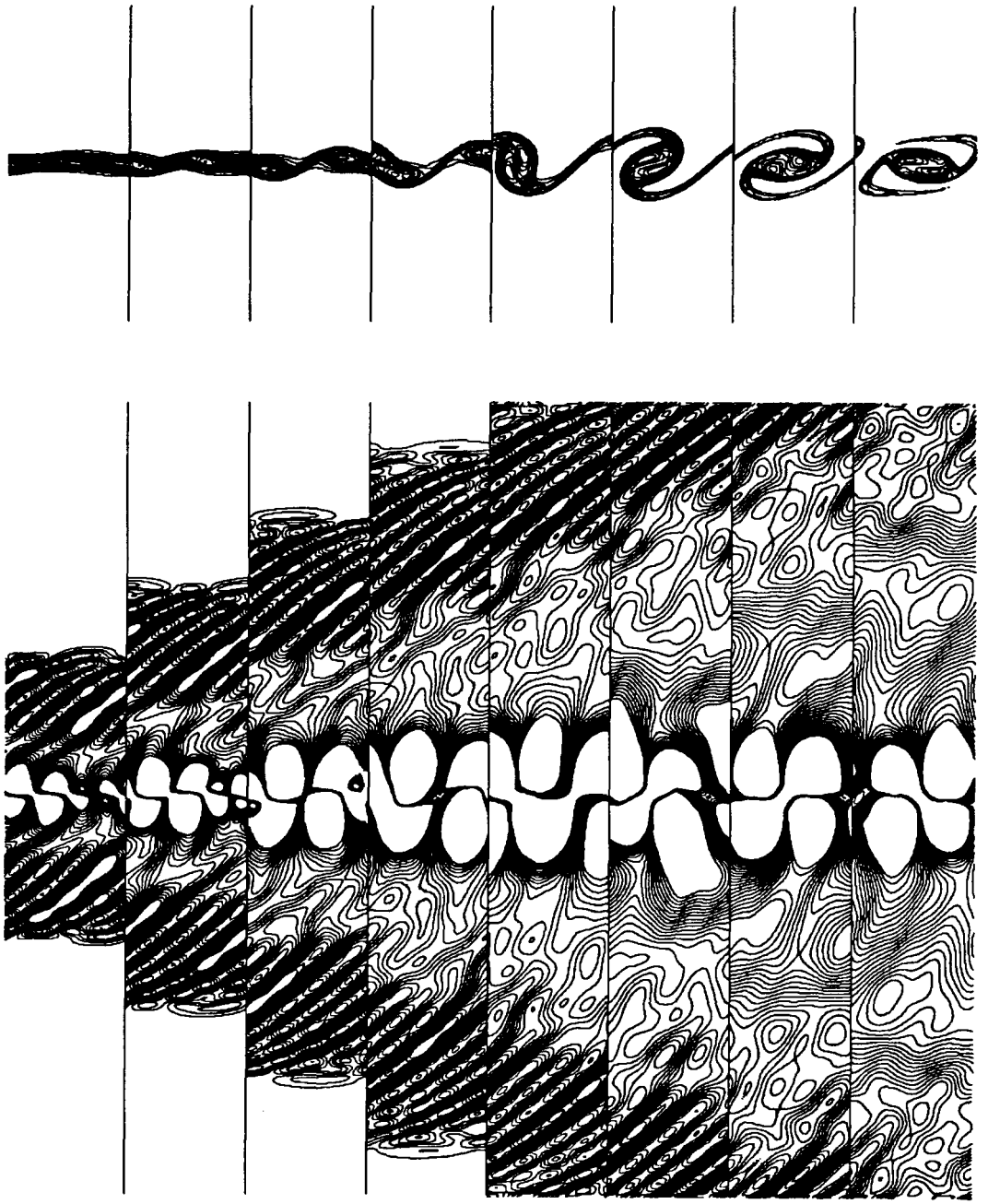

FIGURE 7. Contours of vorticity and dilatation fields. Snapshots from eight equally spaced times are arranged from left to right. The vorticity contours (shown only in a part of the domain) provide a visualization of the flow generating the acoustic waves radiating to the far-field. The plotted dilatation contours are chosen to show the waves in the far-field. Waves generated by the roll up and pairing are preceded by an initial transient.

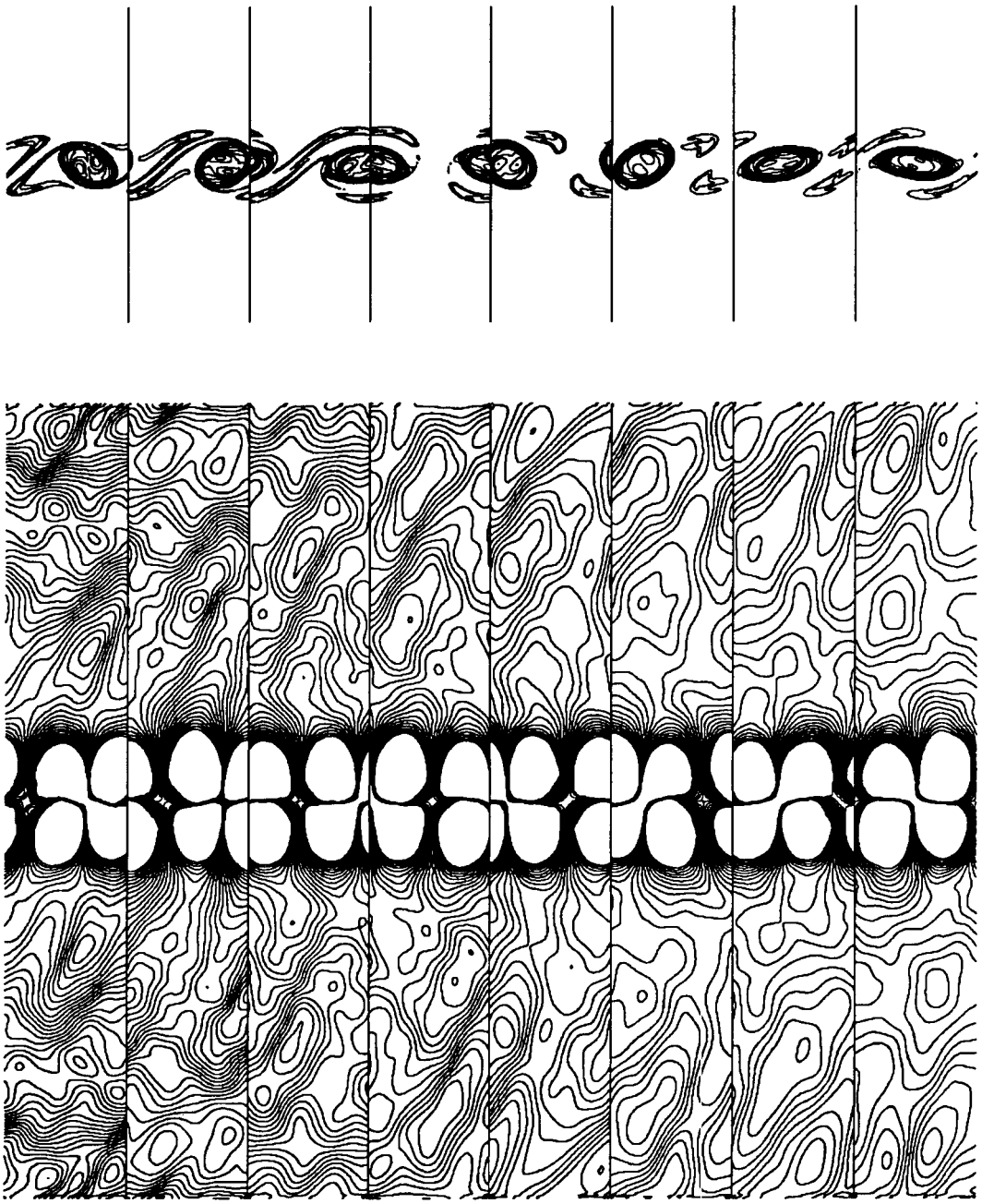

FIGURE 8. Contours of vorticity and dilatation fields. Continuation of the time series in the figures on left. Sound waves generated by the vortex unsteadiness after a vortex merger are shown. Almost two cycles of this unsteadiness are shown.

following the time evolution of vorticity, dilatation and pressure fields during the roll up and pairing events. The roll up process generated a compression wave, while the pairing event generated a compression and an expansion wave. The acoustic power emitted during a pairing was 5-6 times stronger than the emission from a roll up of the fundamental disturbance.

Examples of the time evolution of the vorticity and dilatation fields are shown in figures 7 and 8, respectively. For this case, the velocity ratio $\frac{U_2}{U_1}$ is 0.2 and $T_2 = T_1$, where the subscripts refer to the high and low speed streams. The two streams have Mach numbers of $M_1 = 1.0$ and $M_2 = 0.2$ which corresponds to a convective Mach number (as defined by Papamoschou and Roshko 1986) of $M_c = 0.4$. The calculations are performed in a frame of reference moving with $\frac{U_f}{U_1}$ of 0.4. Note that this reference speed is different from the propagation speed of the vortices, $\frac{U_c}{U_1}$ of 0.6. It was verified that the reference speed had no effect on the results described here. The panels in these figures correspond to 8 different snapshots of the flow as it evolves. The roll up and pairing is evident from the vorticity contours. The dilatation pattern associated with each vortex is a quadrupole, and the acoustic waves radiate during the roll up and vortex merging stage. The vortex merging process generates first a compression wave while the Reynolds stresses extract work from the mean flow. Later in time the Reynolds stress is negative in the shear layer, indicating that energy is being transferred from the shear region back to the mean flow. At the same time, sound is radiated to the surroundings in the form of an expansion wave.

In the far-field the density, pressure and velocity fluctuations were computed. The acoustic energy flux radiated to the far-field was also monitored. It was found that the far-field fluctuations satisfied plane wave acoustic relations exceedingly well. The fluctuations in the near-field (pressure and velocity) were found to decay exponentially away from the shear layer. This near-field region was found to scale with the hydrodynamic instability wavelength.

In the future the Mach number dependence of the radiated acoustic flux will be studied, and acoustic radiation from spatially-evolving mixing layers will be studied.

Acknowledgement

The first two authors (C.M.H. & Y.Z.) wish to acknowledge the generous support of the Center for Turbulence Research for making this work possible. This work was partially supported by ONR.

REFERENCES

BERNAL, L. P. & ROSHKO, A. 1986 Streamwise Vortex Structure in Plane Mixing Layers. *J. Fluid Mech.* **170**, 499–525.

CAIN, A. B., FERZIGER, J. H. & REYNOLDS, W. C. 1984 Discrete Orthogonal Function Expansions for Non-uniform Grids Using the Fast Fourier Transform. *J. Comp. Phys.* **56**, 272–286.

HO, C. M. & HUERRE, P. 1984 Perturbed Free Shear Layers. *Ann. Rev. Fluid Mech.* **16**, 365–424.

HUANG, L. S. & HO, C. M. 1988 Small-Scale Transition in Plane Mixing Layers. *in preparation.*

KONRAD, J. H. 1976 An Experimental Investigation of Mixing in Two-Dimensional Turbulent Shear Flows with Applications to Diffusion-Limited Chemical Reactions. *Intern. Rep. CIT-8-PU,* Calif. Inst. Tech., Pasadena.

LAUFER, J. 1974 On the Mechanism of Noise Generation by Turbulence. In *Omaggio a Carlo Ferrari*p. 451, Libreria Editrice Universitaria Levrotto and Bella, Torino.

PAPAMOSCHOU, D.& ROSHKO, A. 1986 Observations of Supersonic Free Shear Layers. *AIAA Paper 86-0162.*

PIERREHUMBERT, R. T. & WIDNALL, S. E. 1982 The Two- and Three-Dimensional Instabilities of a Spatially Periodic Shear Layer. *J. Fluid Mech.* **114**, 59-82.

STUART, J. T. 1967 On Finite Amplitude Oscillations in Laminar Mixing Layers. *J. Fluid Mech.* **29**, 417-440.

ZOHAR, Y., FOSS, J. K., HO, C. M. & BUELL, J. C. 1988 Phase De-correlation in Plane Mixing Layers. in preparation.